Electronic Supplementary Material (ESI) for Inorganic Chemistry Frontiers.

Electronic Supplementary Information

for the manuscript entitled

Cobalt Mediated *N*-Alkylation of Amines by Alcohols: Role of Hydrogen Bonding Pocket

Divya Prabha, Sanya Pachisia and Rajeev Gupta*

Department of Chemistry, University of Delhi, Delhi 110007 (India)

E-mail: *rgupta@chemistry.du.ac.in*

List of Figures:

List of Tables:

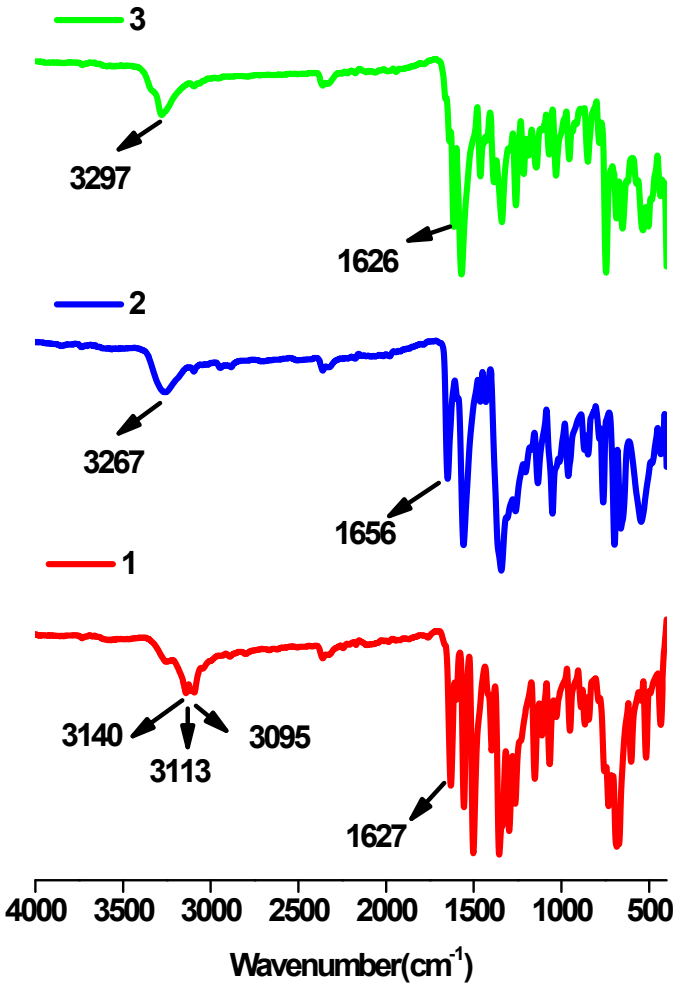

Figure S1. FTIR spectra of **1** (red trace), **2** (blue trace) and **3** (green trace) recorded at 25 °C.

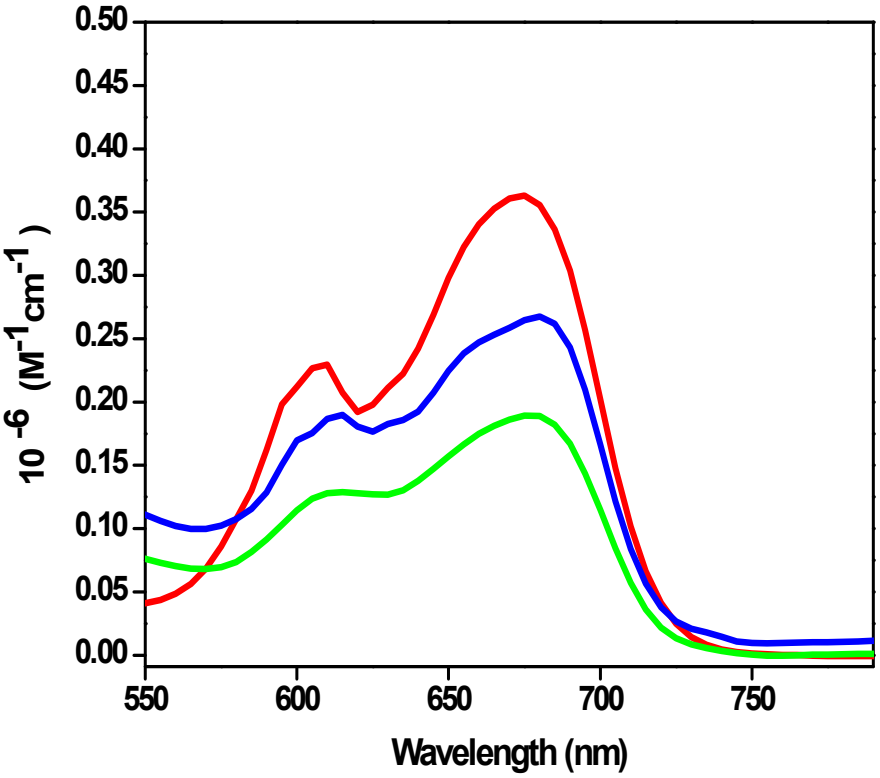

Figure S2. UV-Visible spectra of **1–3** (ca. 50μM) recorded in DMF at 25 °C.

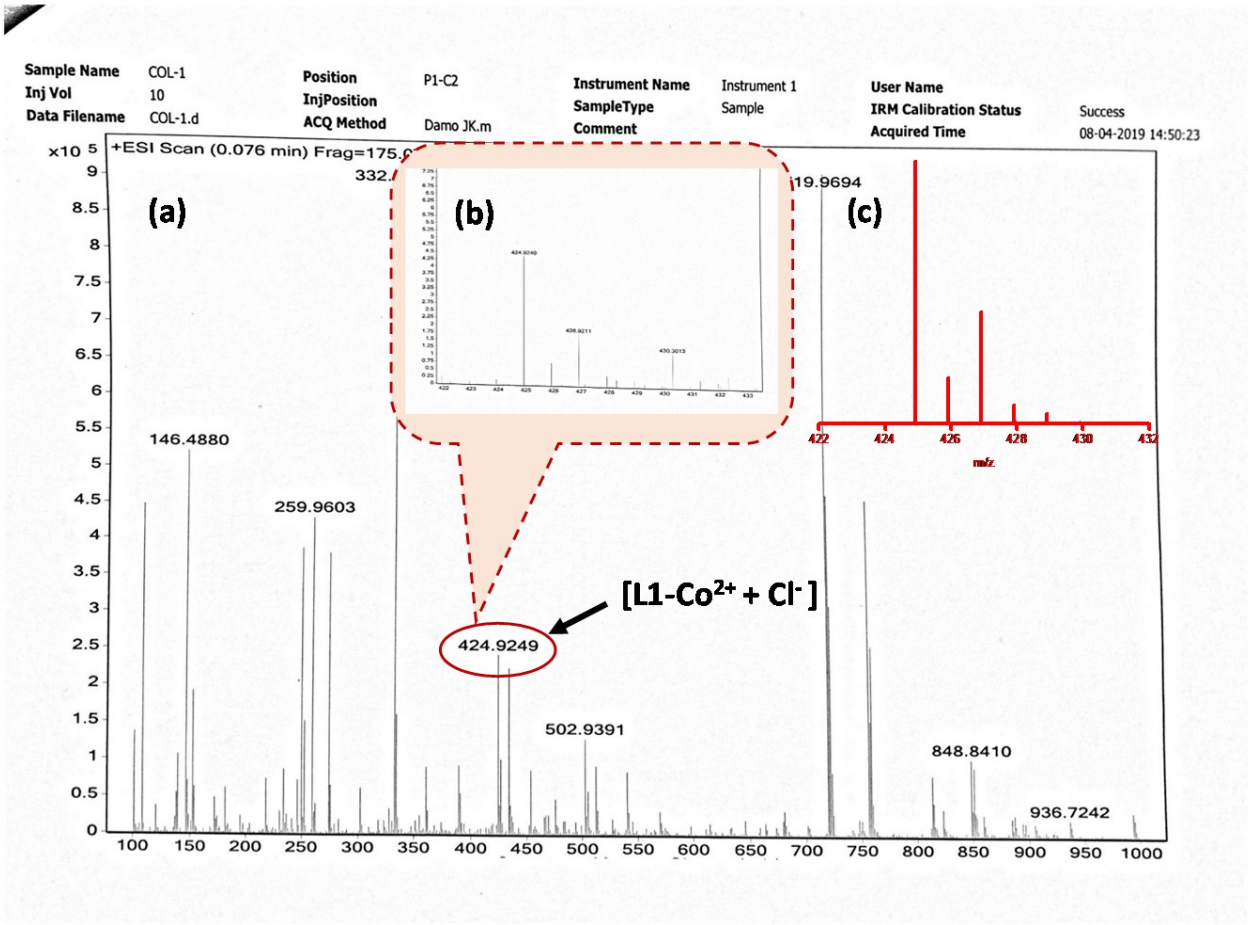

Figure S3. (a) Full range ESI^{+}-MS spectrum of **1** recorded in DMF. (b and c) Comparison of the relevant isotope pattern with the simulated pattern calculated using ChemCalc.

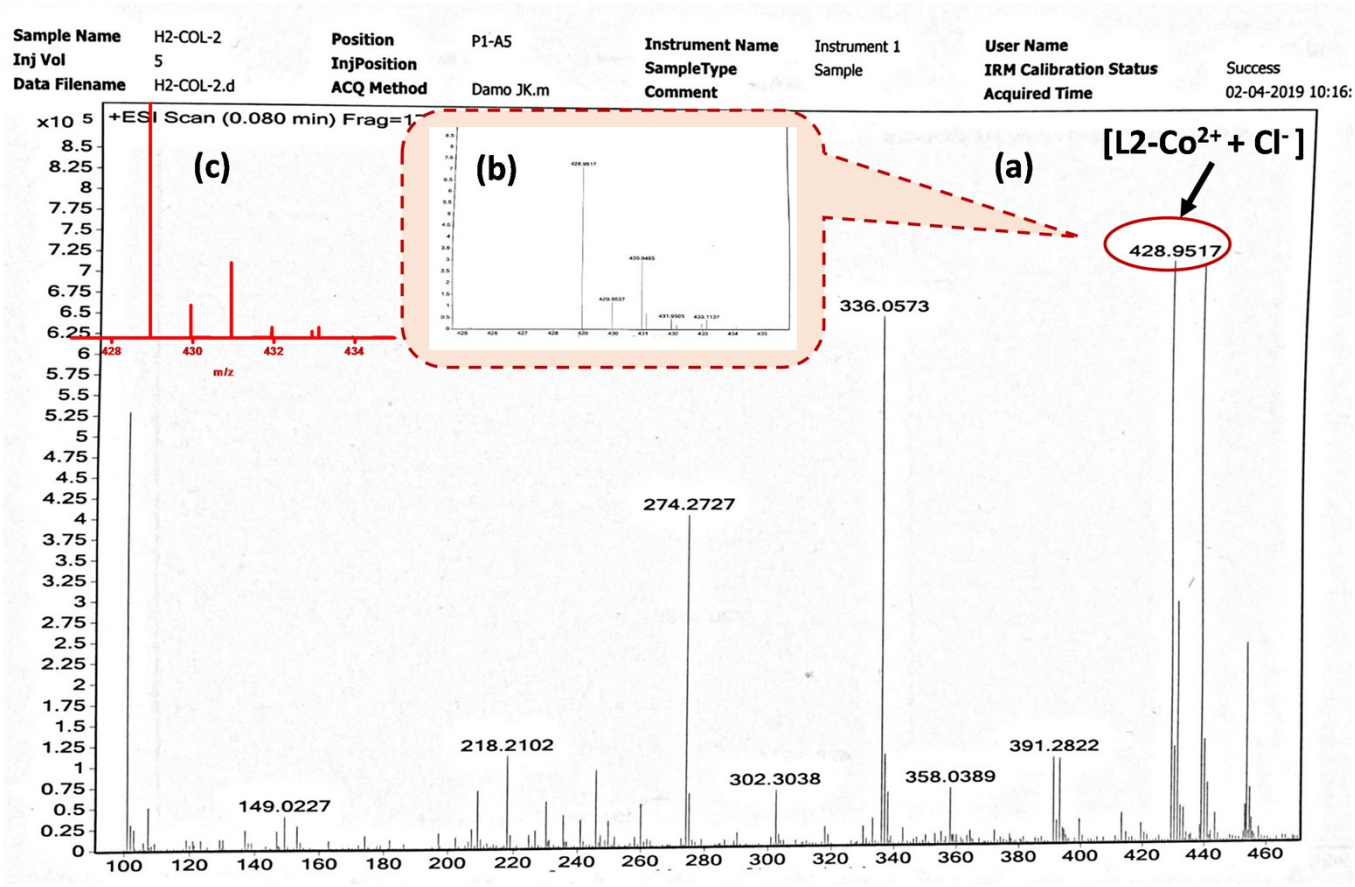

Figure S4. (a) Full range ESI^{+}-MS spectrum of **2** recorded in DMF. (b and c) Comparison of the relevant isotope pattern with the simulated pattern calculated using ChemCalc.

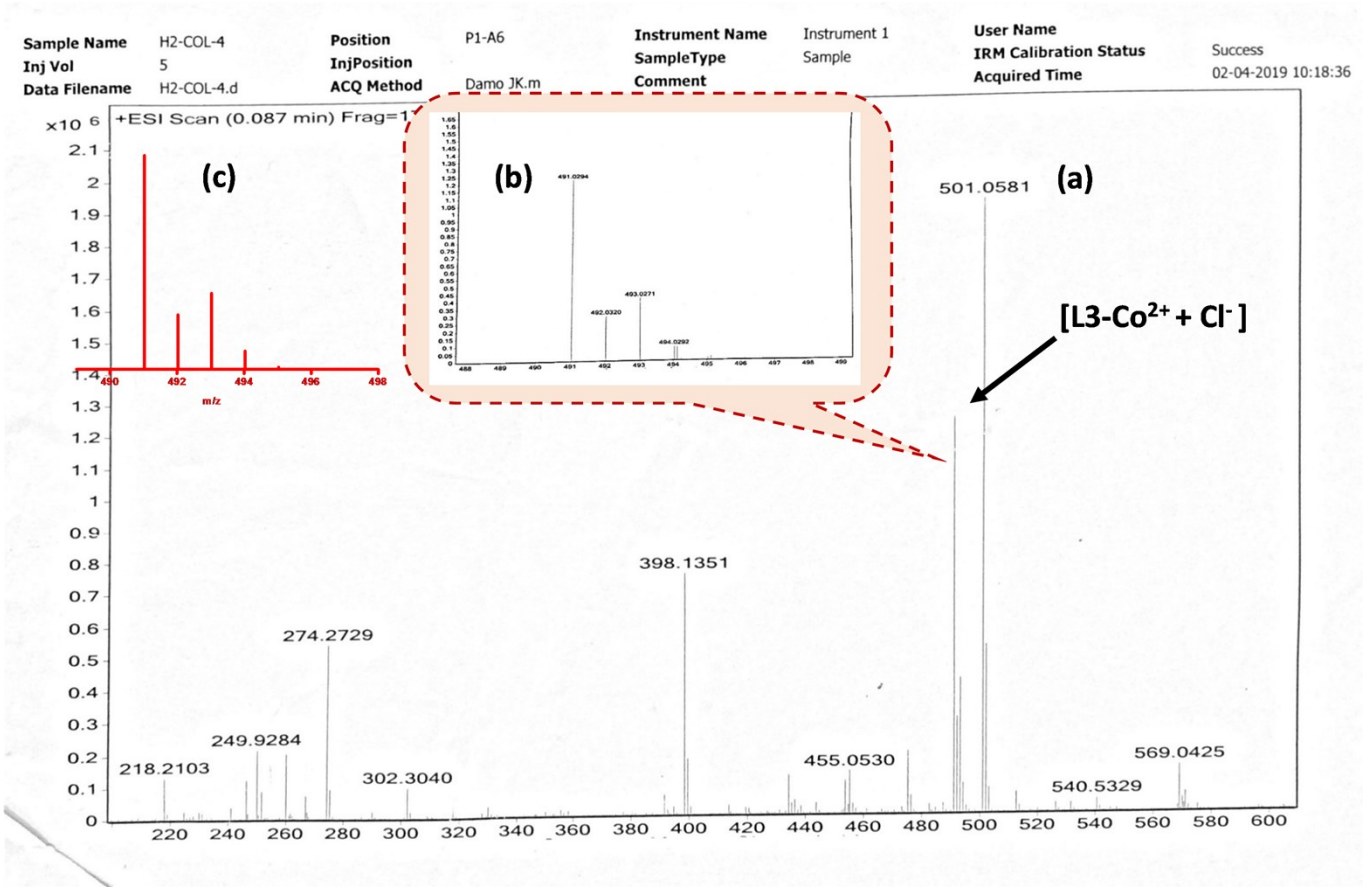

Figure S5. (a) Full range ESI^{+}-MS spectrum of **3** recorded in DMF. (b and c) Comparison of the relevant isotope pattern with the simulated pattern calculated using ChemCalc.

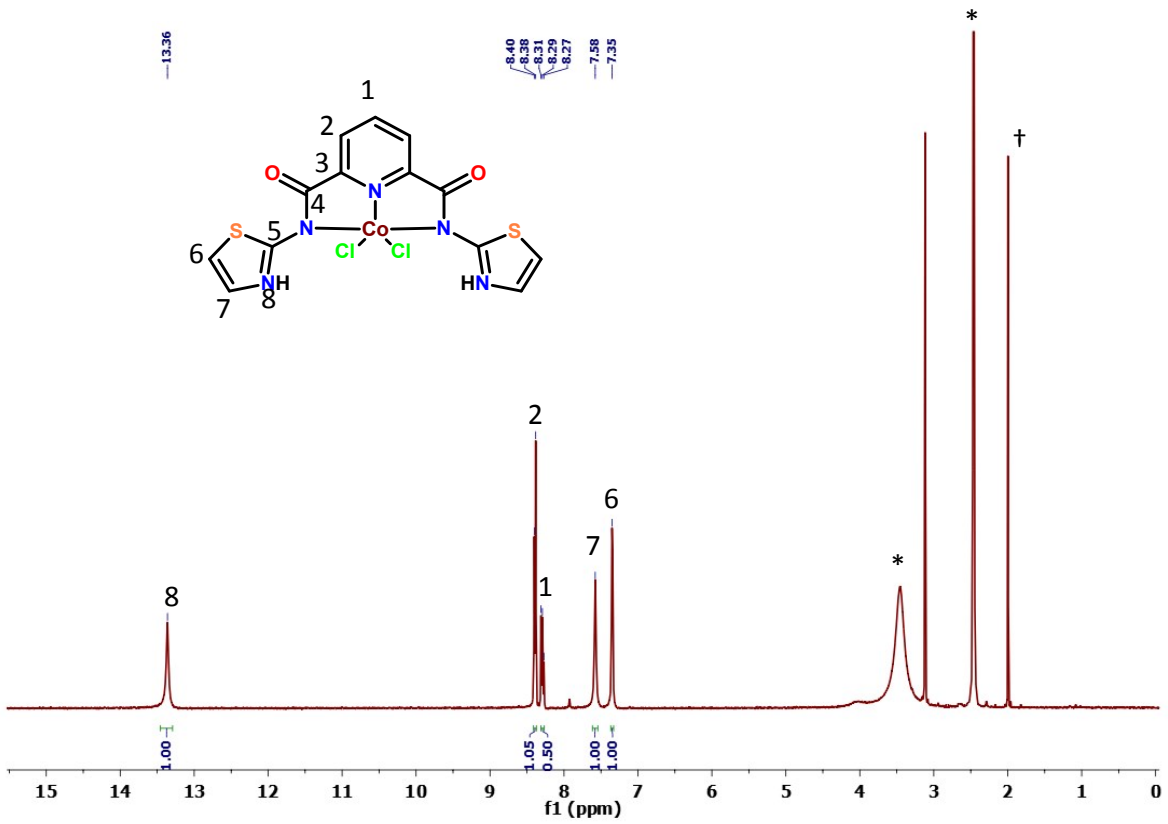

Figure S6. ^{1}H NMR (400 MHz, DMSO-D_6, 25 °C) spectrum of **1**. Asterisk represents the residual solvent and adventitious water while † represents the peak for acetonitrile.

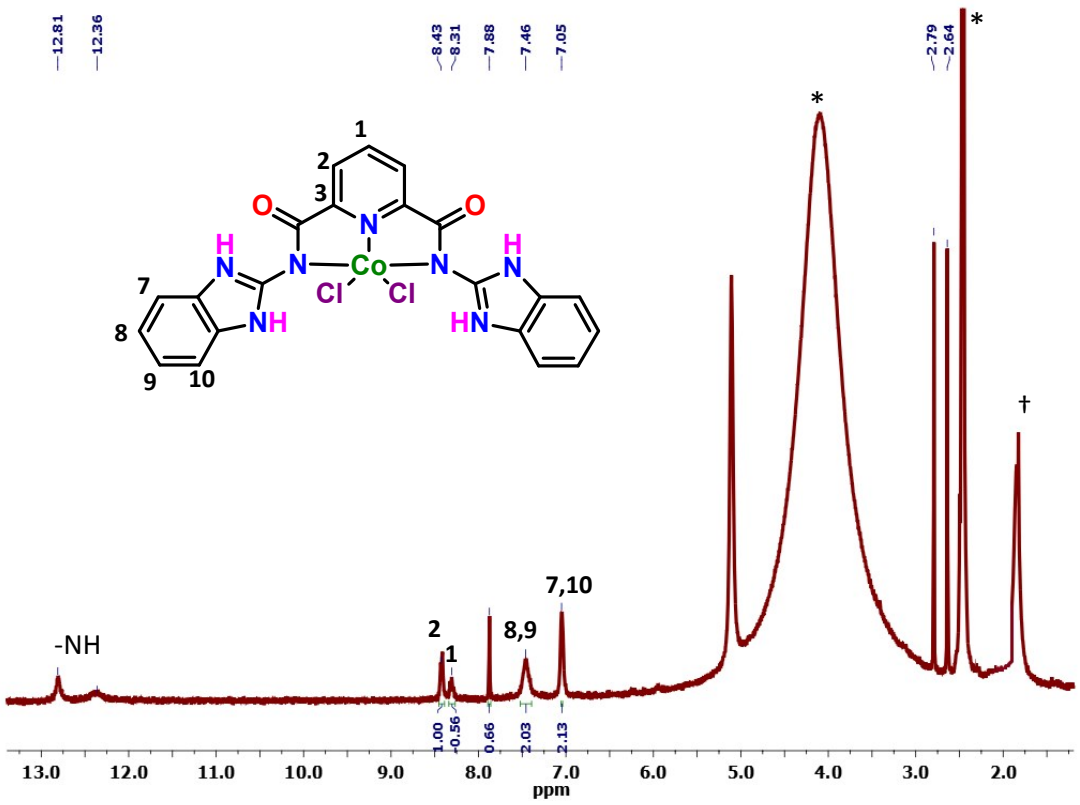

Figure S7. ^{1}H NMR (400 MHz, DMSO-D_6, 25 °C) spectrum of **3**. Asterisk represents the residual solvent and adventitious water while † represents the peak for acetonitrile. Peaks at 2.64, 2.79 and 7.88 ppm are due to residual DMF.

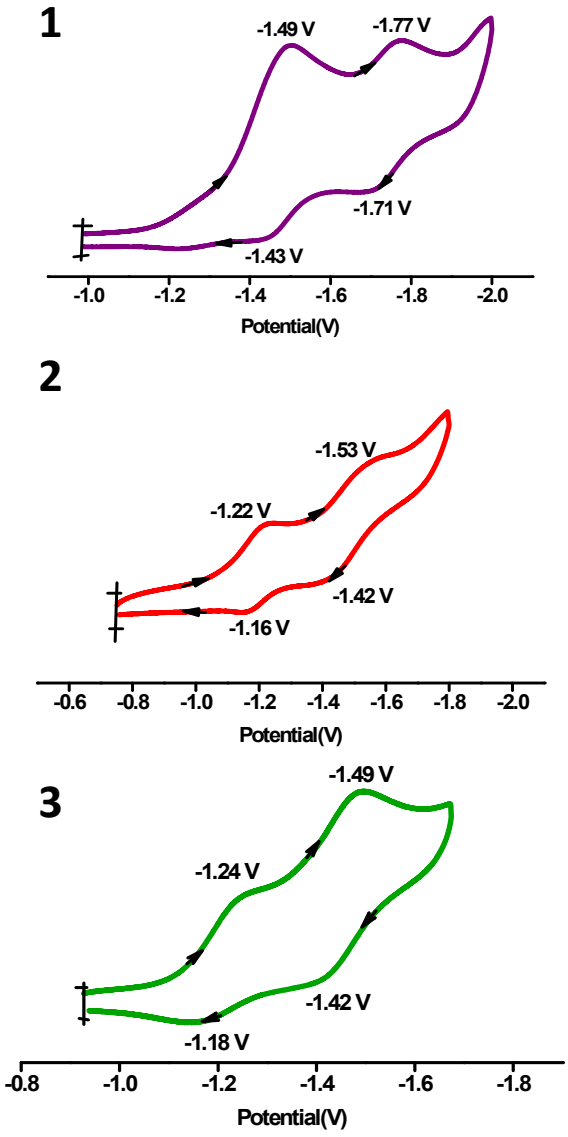

Figure S8. Cyclic voltammograms (negative potential region) of **1** (purple trace), **2** (red trace) and **3** (green trace) recorded in DMF at 25 °C. Conditions: cobalt complex (ca. 1 mM); supporting electrolyte, TBAP (ca. 100 mM); working electrode, glassy carbon; reference electrode, Ag/Ag^{+}; auxiliary electrode, Pt wire; scan rate, 100 mV/s.

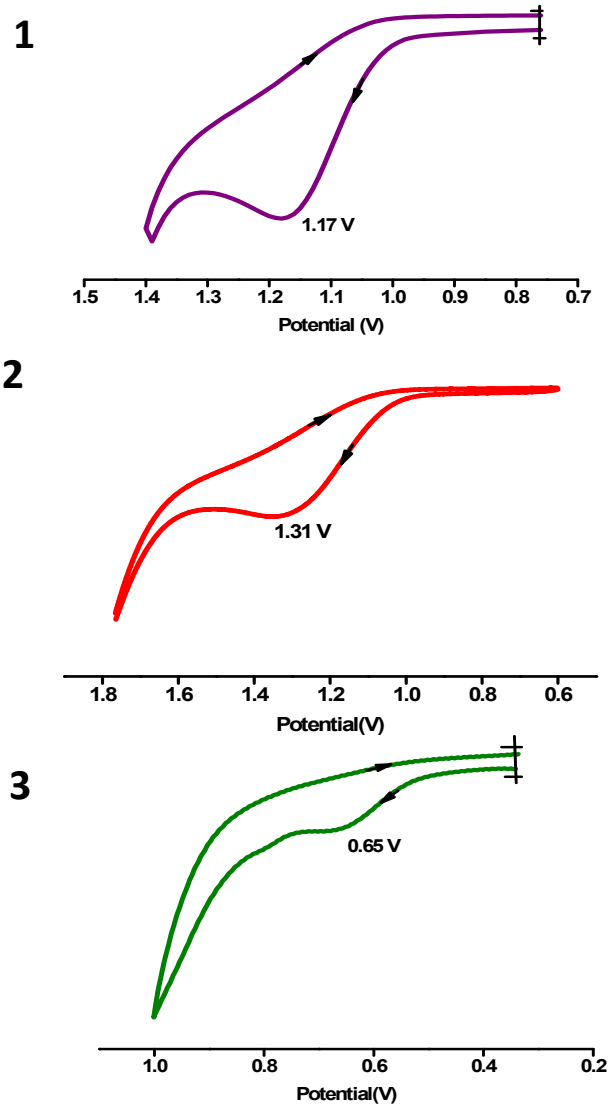

Figure S9. Cyclic voltammograms (positive potential region) of **1** (purple trace), **2** (red trace) and **3** (green trace) recorded in DMF at 25 °C. Conditions: cobalt complex (ca. 1 mM); supporting electrolyte, TBAP (ca. 100 mM); working electrode, glassy carbon; reference electrode, Ag/Ag^{+}; auxiliary electrode, Pt wire; scan rate, 100 mV/s.

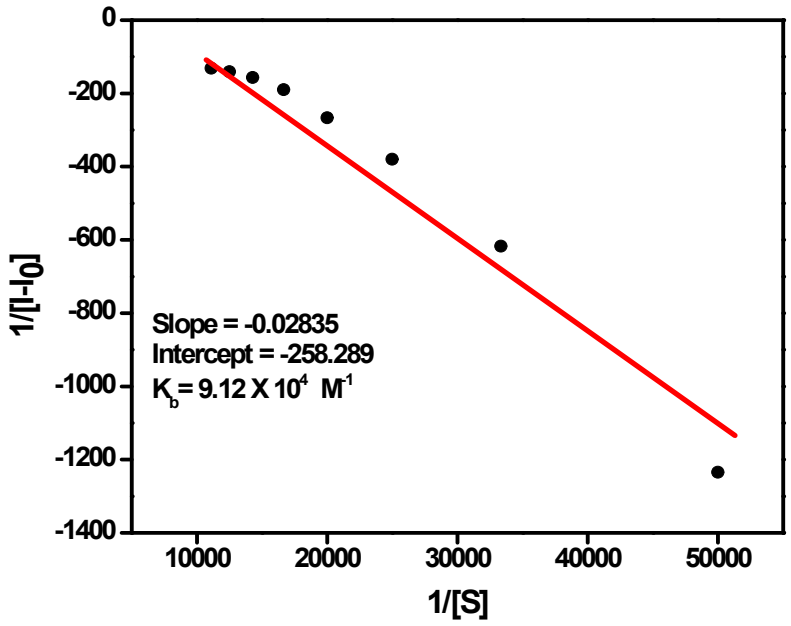

Figure S10. Benesi-Hildebrand plot for the binding of 4-methoxy benzyl alcohol with **1** using the UV-Visible spectral titration at 30 °C.

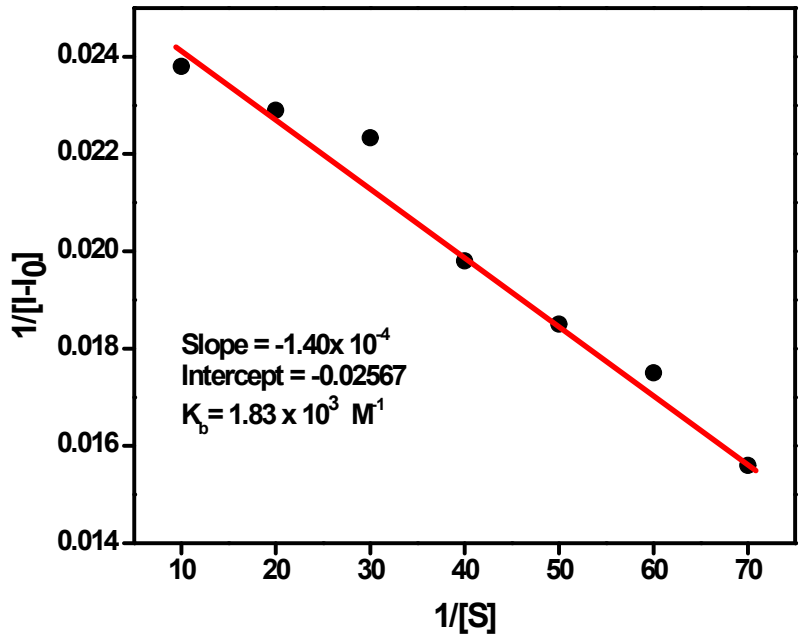

Figure S11. Benesi-Hildebrand plot for the binding of 4-nitro-benzyl alcohol with **1** using the UV-Visible spectral titration at 30 °C.

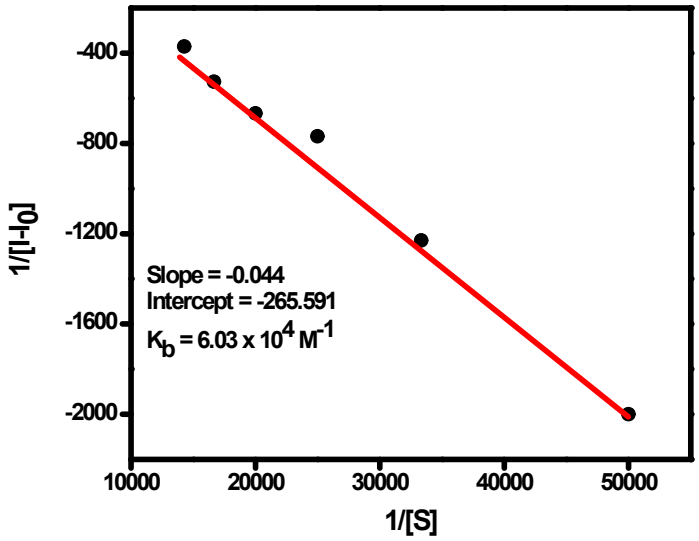

Figure S12. Benesi-Hildebrand plot for the binding of benzyl alcohol with **1** using the UV-Visible spectral titration at 40 °C.

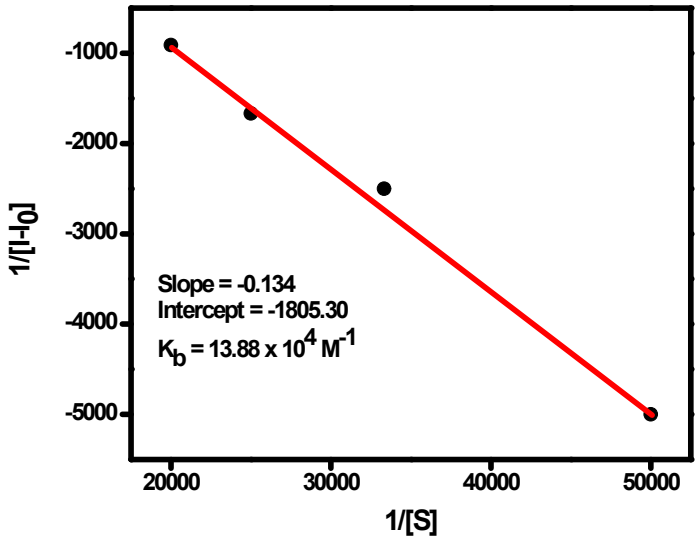

Figure S13. Benesi-Hildebrand plot for the binding of benzyl alcohol with **1** using the UV-Visible spectral titration at 50 °C.

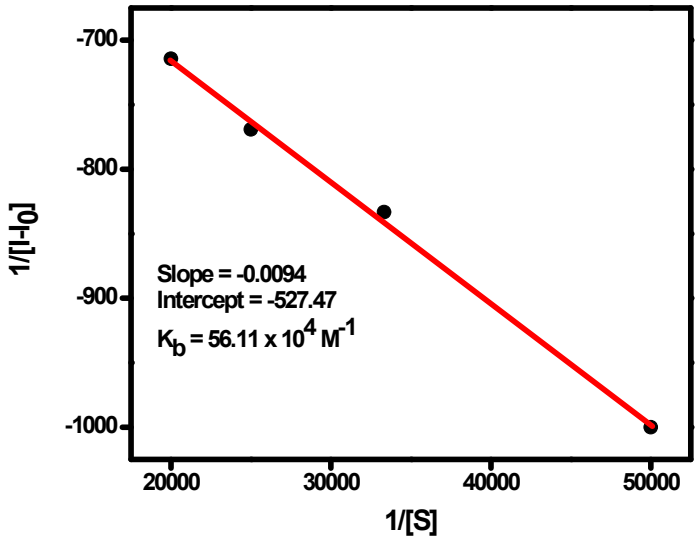

Figure S14. Benesi-Hildebrand plot for the binding of benzyl alcohol with **1** using the UV-Visible spectral titration at 60 °C.

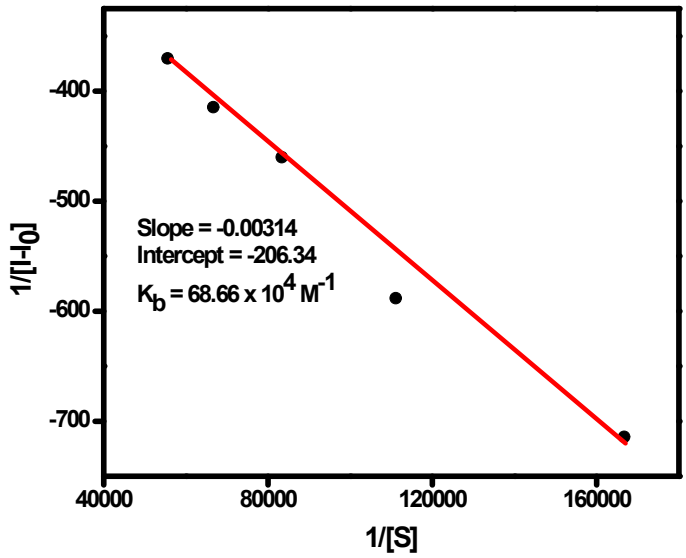

Figure S15. Benesi-Hildebrand plot for the binding of benzyl alcohol with **1** using the UV-Visible spectral titration at 70 °C.

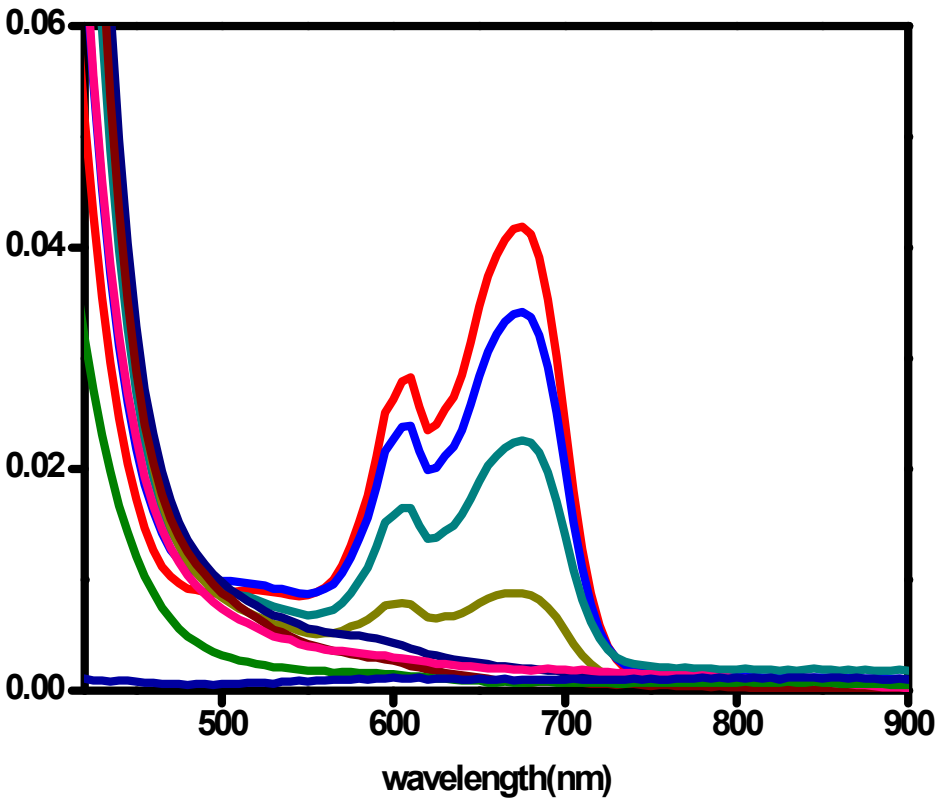

Figure S16. Change in the absorption spectra of **1** with increasing concentration of potassium salt of benzyl alcohol recorded in DMF at 25 °C.

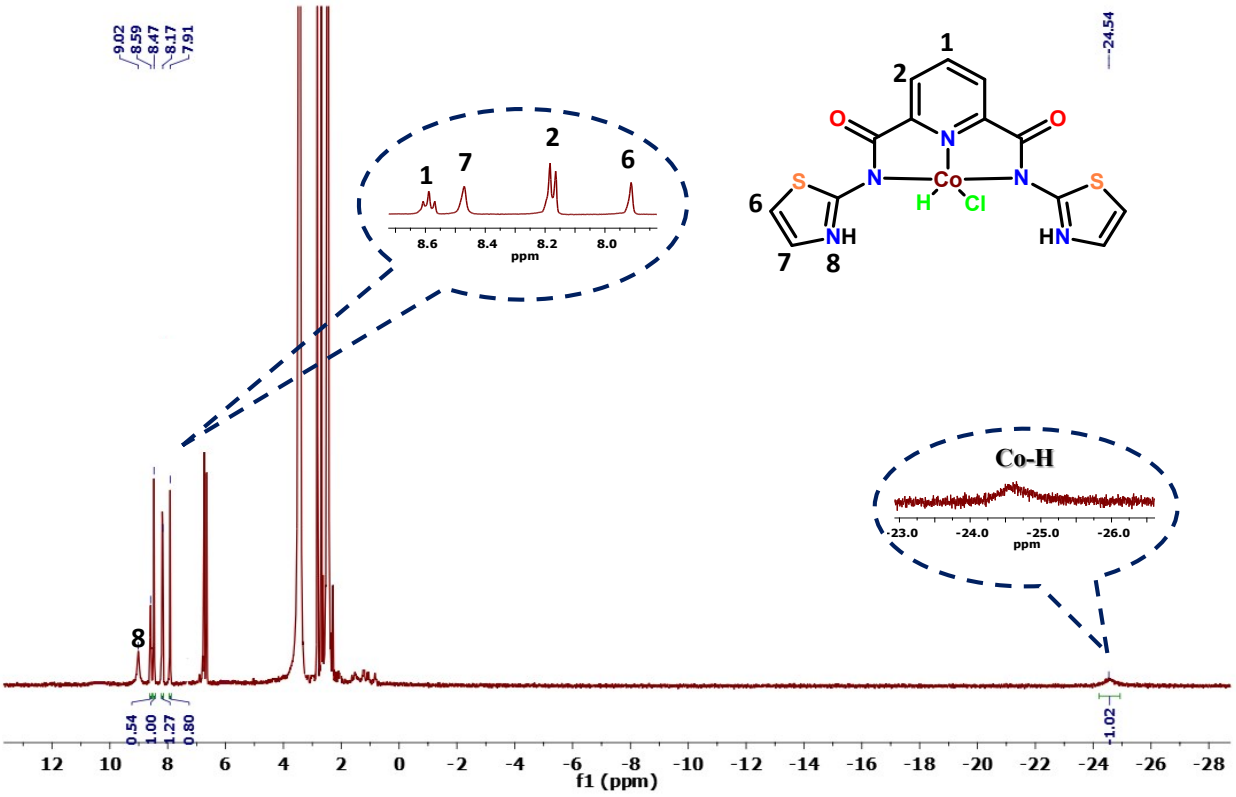

Figure S17. ^{1}H NMR (400 MHz, DMSO-D_6, 25 °C) spectrum of **1** on addition of benzyl alcohol and KOH. The magnified view in the negative ppm region shows the peak for the in-situ generated Co-hydride species.

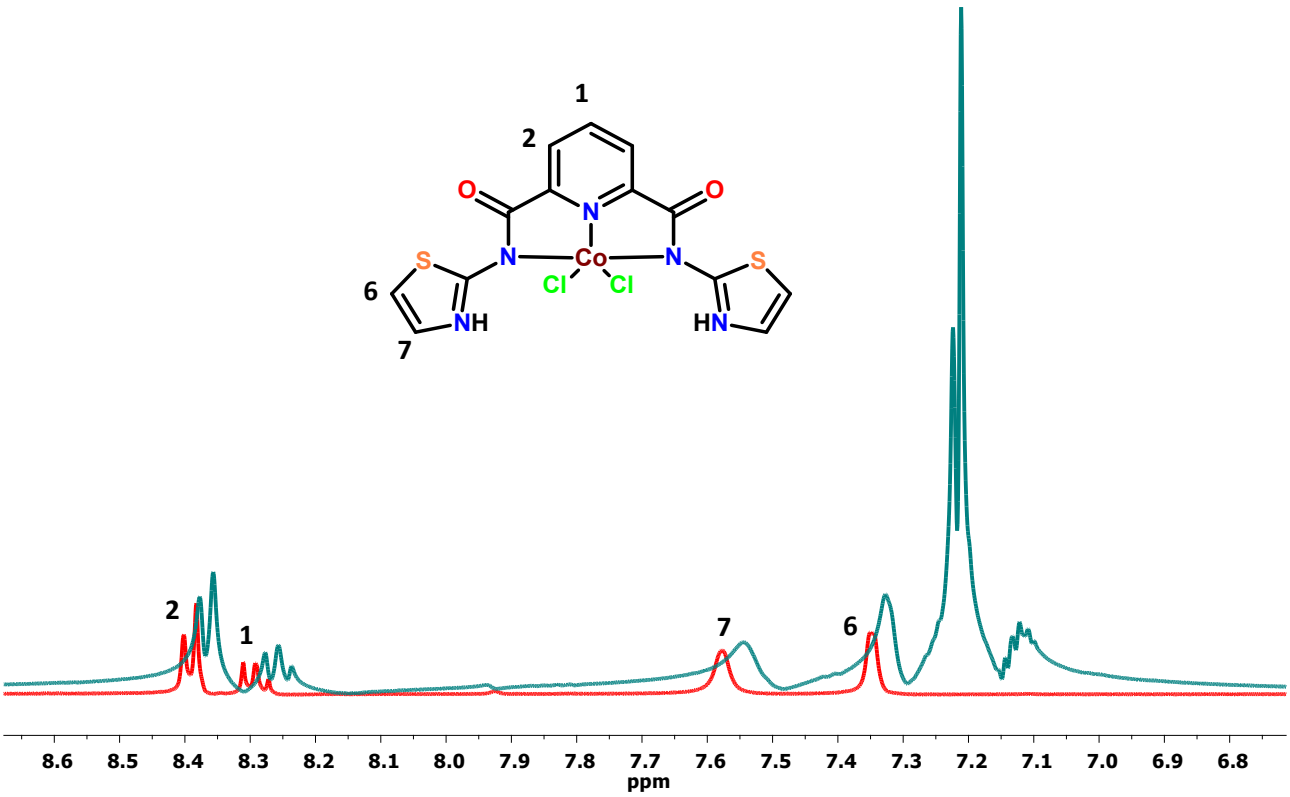

Figure S18. Comparison of the selected parts of ^{1}H NMR (400 MHz, DMSO-D_6, 25 °C) spectra of **1** (red trace) and the one after the addition of benzyl alcohol (blue trace). The resonances at ca. 7.1 and ca. 7.2 ppm are due to excess of benzyl alcohol.

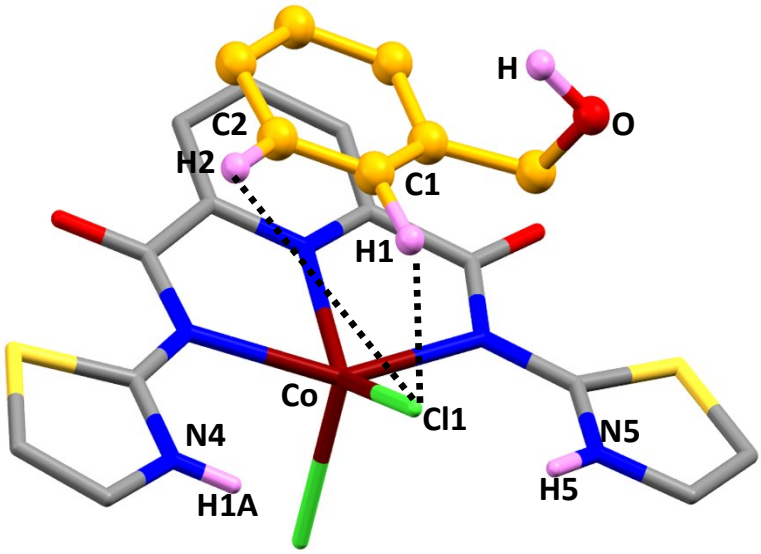

Figure S19. Docking structure of **1** to that of benzyl alcohol (carbon atoms are shown in golden color for clarity). The arene-hydrogen atoms of benzyl alcohol show weak interactions to that of one of the Co-coordinated chlride atoms. Heteroatom separations for the selected H-bonds; C1-H1…Cl1: 2.94 – 3.33 Å and C2-H2…Cl1: 3.02 – 3.69 Å.

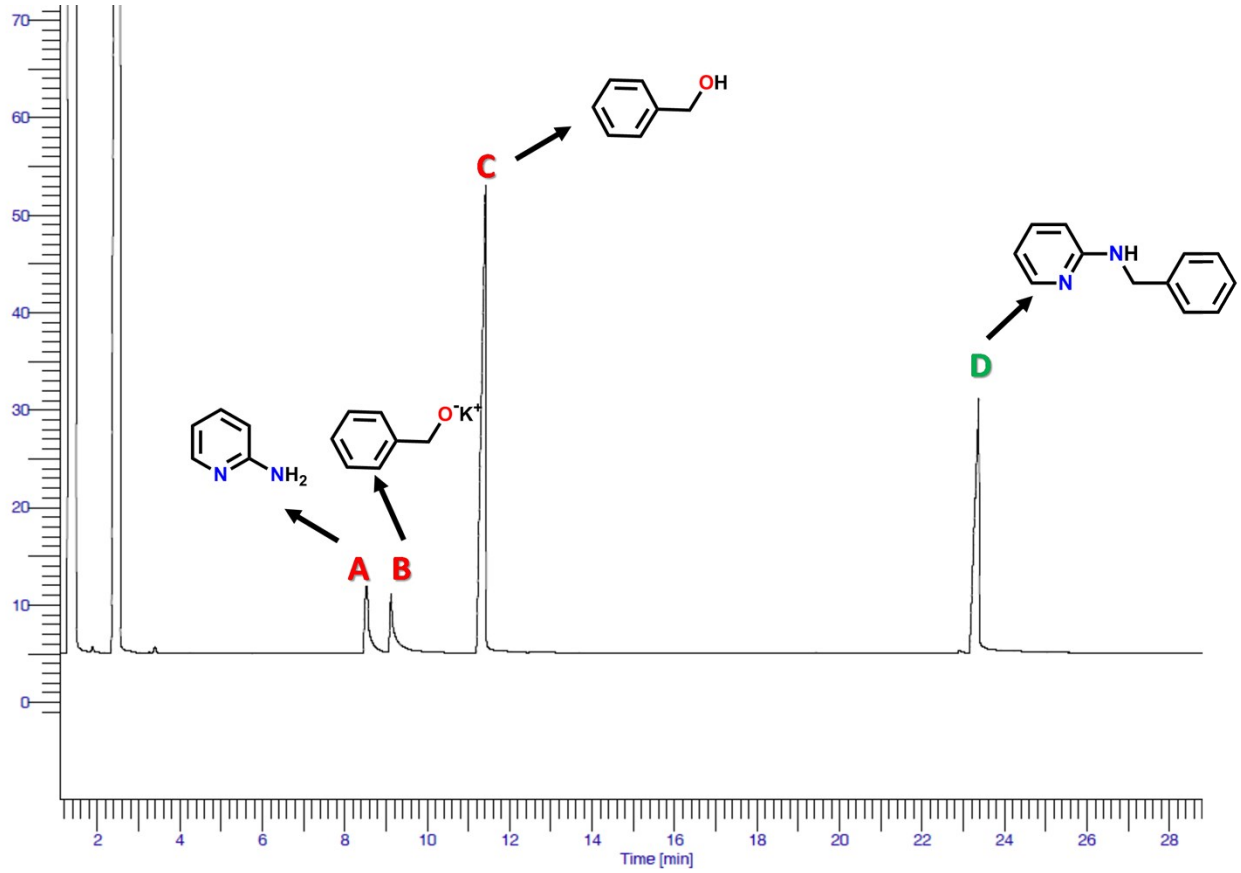

Figure S20. Chromatogram for the *N*-alkylation of 2-aminopyridine (**A**) with benzyl alcohol (**C**) giving product (**D**) using ligand H_2L^1 and $CoCl_2$.

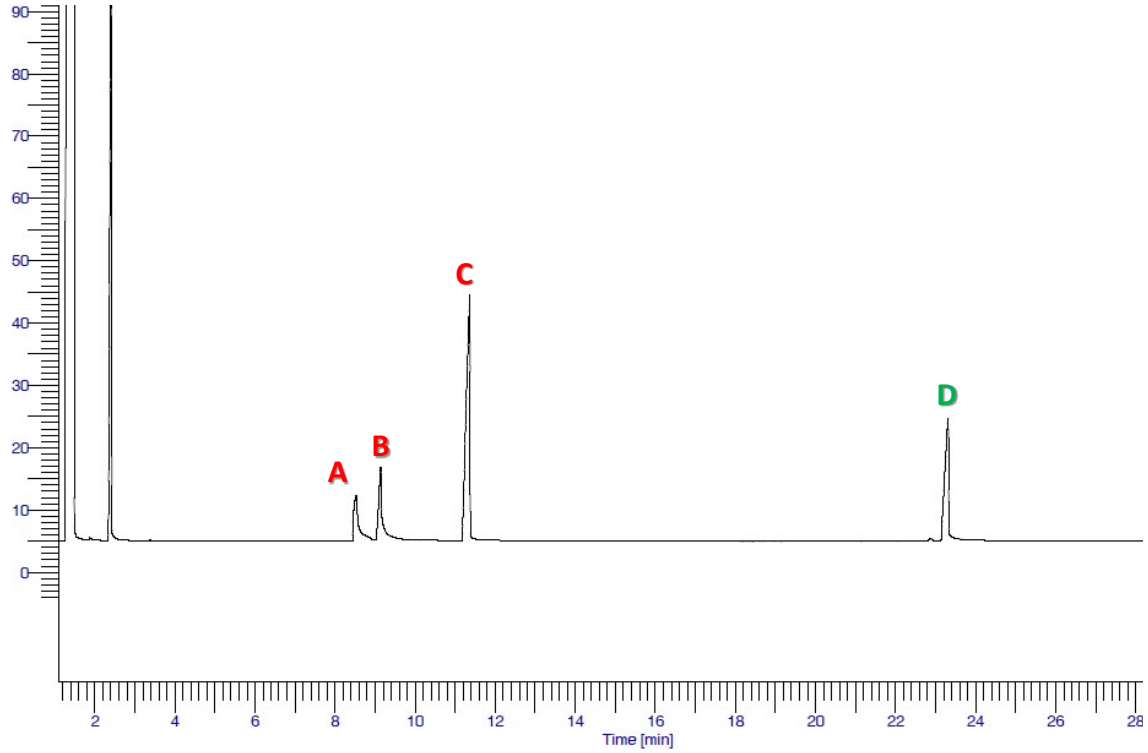

Figure S21. Chromatogram for the *N*-alkylation of 2-aminopyridine (**A**) with benzyl alcohol (**C**) giving product (**D**) using ligand H_2L^2 and $CoCl_2$.

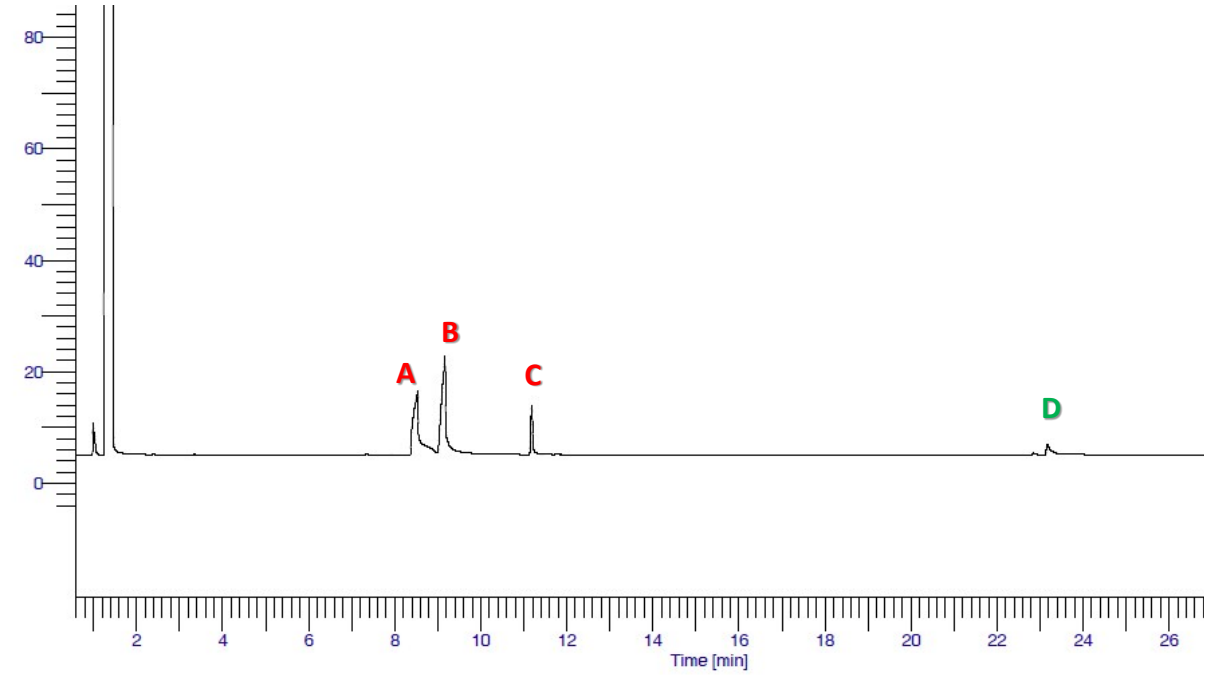

Figure S22. Chromatogram for the *N*-alkylation of 2-aminopyridine (**A**) with benzyl alcohol (**C**) giving product (**D**) using ligand H_2L^4 and $CoCl_2$.

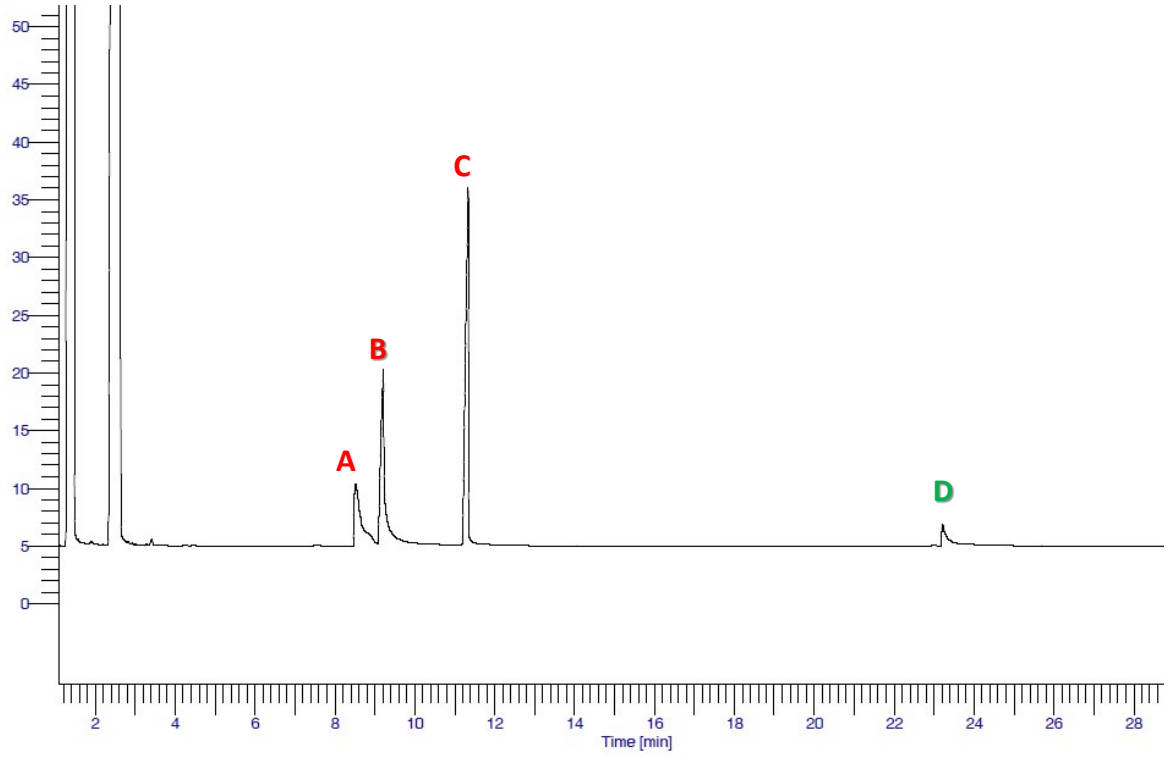

Figure S23. Chromatogram for the *N*-alkylation of 2-aminopyridine (**A**) with benzyl alcohol (**C**) giving product (**D**) using ligand H_2L^5 and $CoCl_2$.

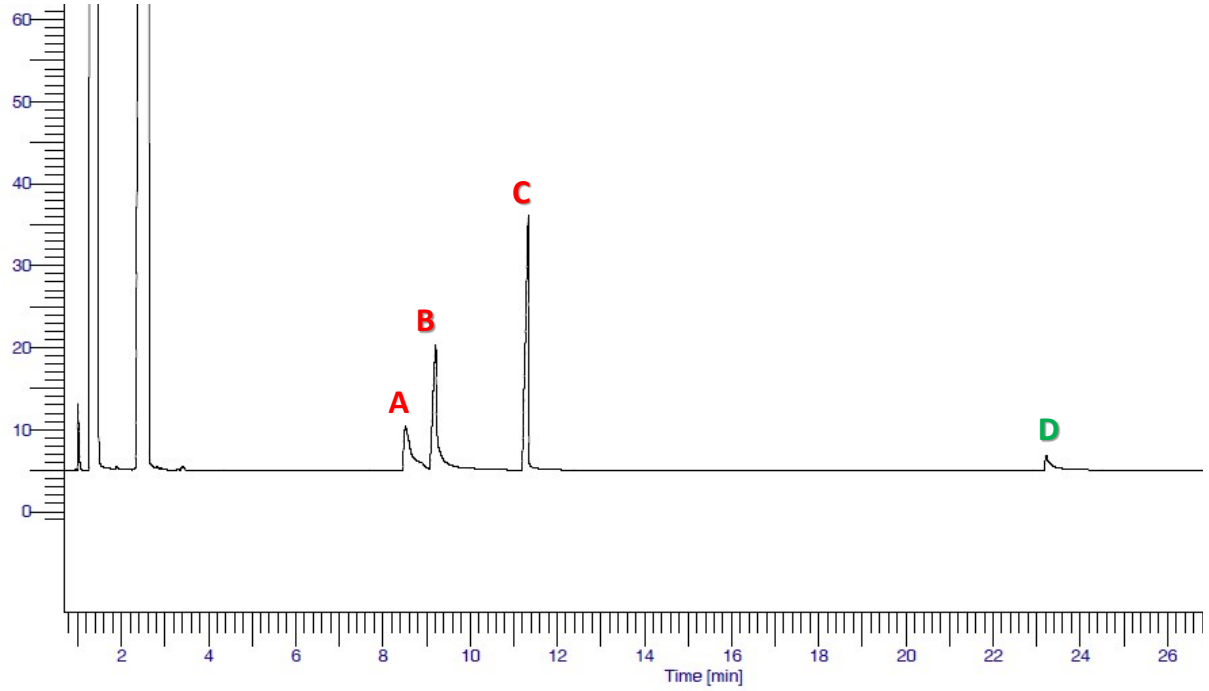

Figure S24. Chromatogram for the *N*-alkylation of 2-aminopyridine (**A**) with benzyl alcohol (**C**) giving product (**D**) using ligand H_2L^6 and $CoCl_2$.

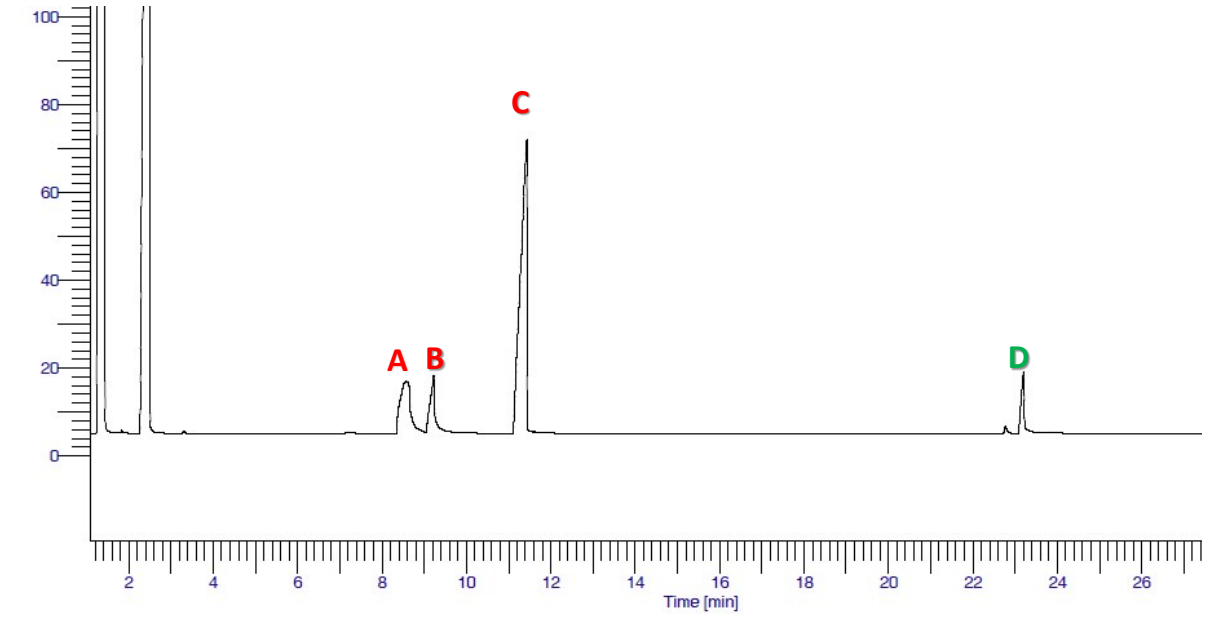

Figure S25. Chromatogram for the *N*-alkylation of 2-aminopyridine (**A**) with benzyl alcohol (**C**) giving product (**D**) using ligand H_2L^7 and $CoCl_2$.

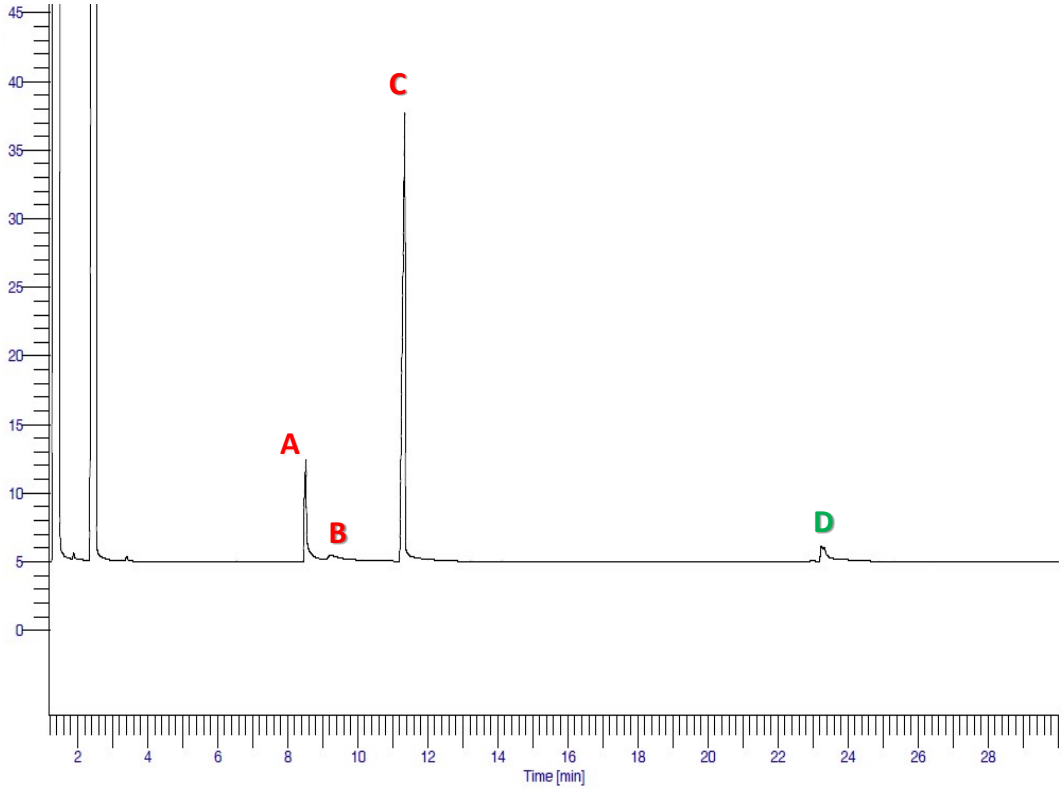

Figure S26. Chromatogram for the *N*-alkylation of 2-aminopyridine (**A**) with benzyl alcohol (**C**) giving product (**D**) using ligand H_2L^8 and $CoCl_2$.

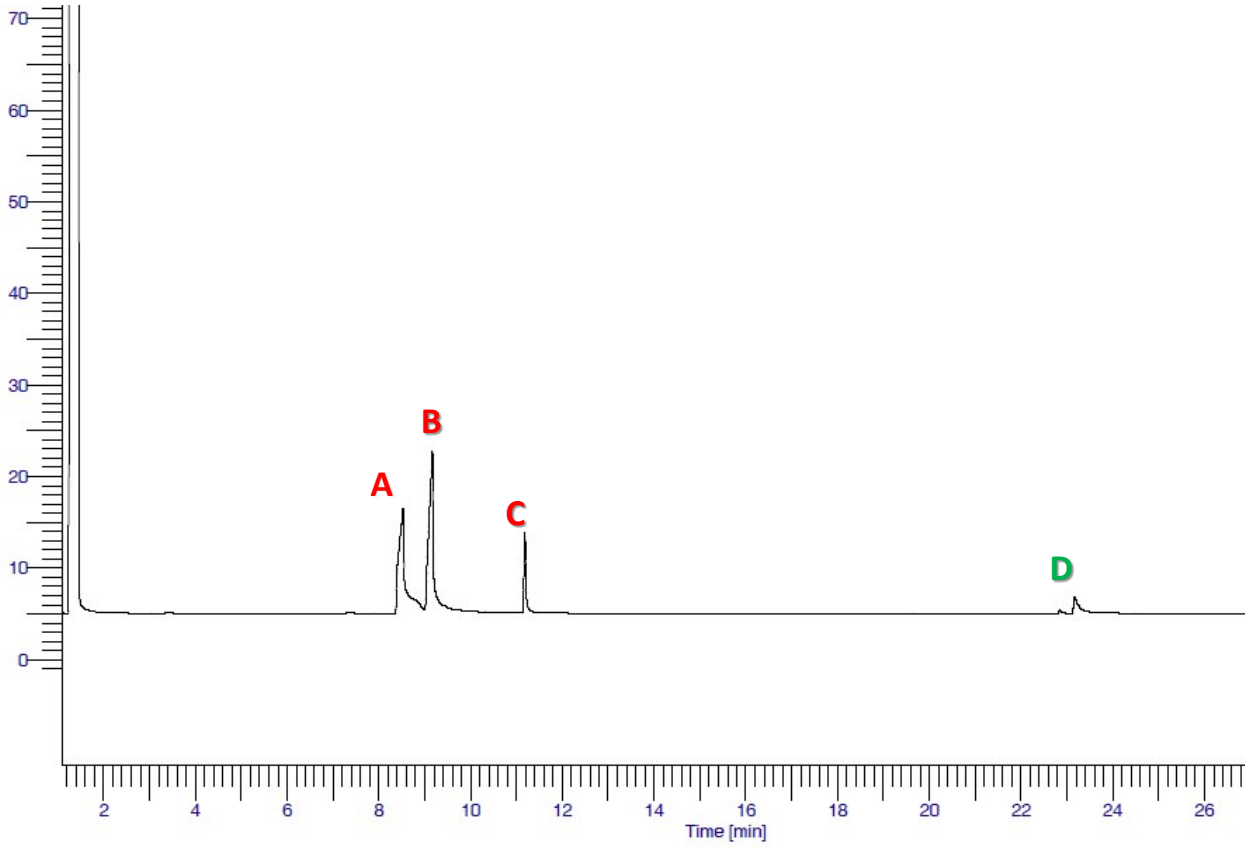

Figure S27. Chromatogram for the *N*-alkylation of 2-aminopyridine (**A**) with benzyl alcohol (**C**) giving product (**D**) using ligand H_2L^9 and $CoCl_2$.

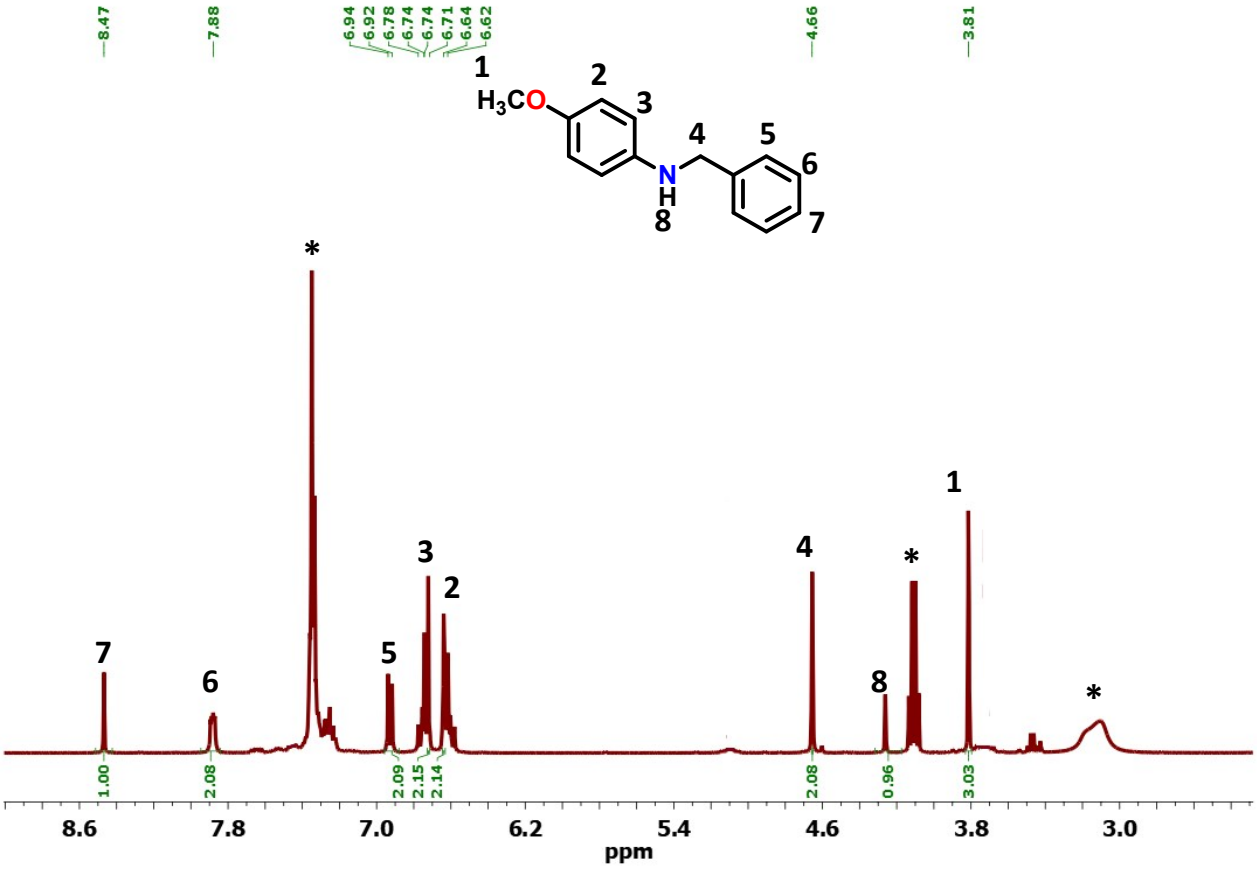

Figure S28. ^{1}H NMR (400 MHz, $CDCl_3$, 25 °C) spectrum of **2g**. Asterisk represents the residual solvents and adventitious water.

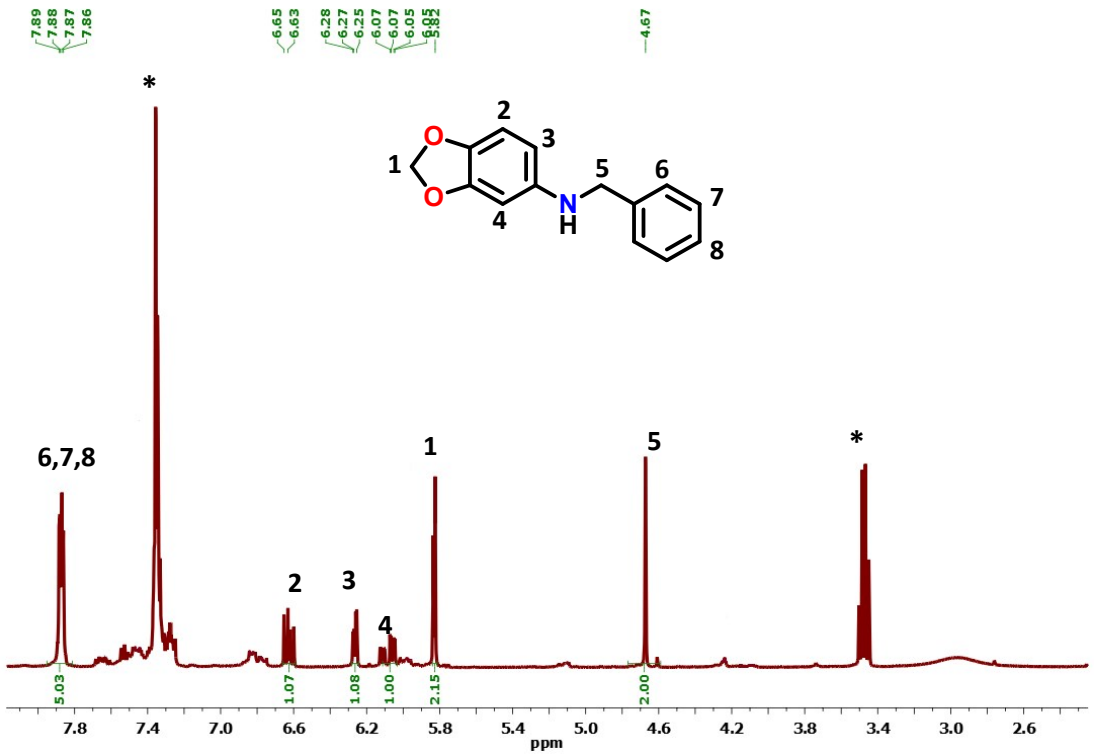

Figure S29. ^{1}H NMR (400 MHz, $CDCl_3$, 25 °C) spectrum of **2d**. Asterisk represents the residual solvents and adventitious water.

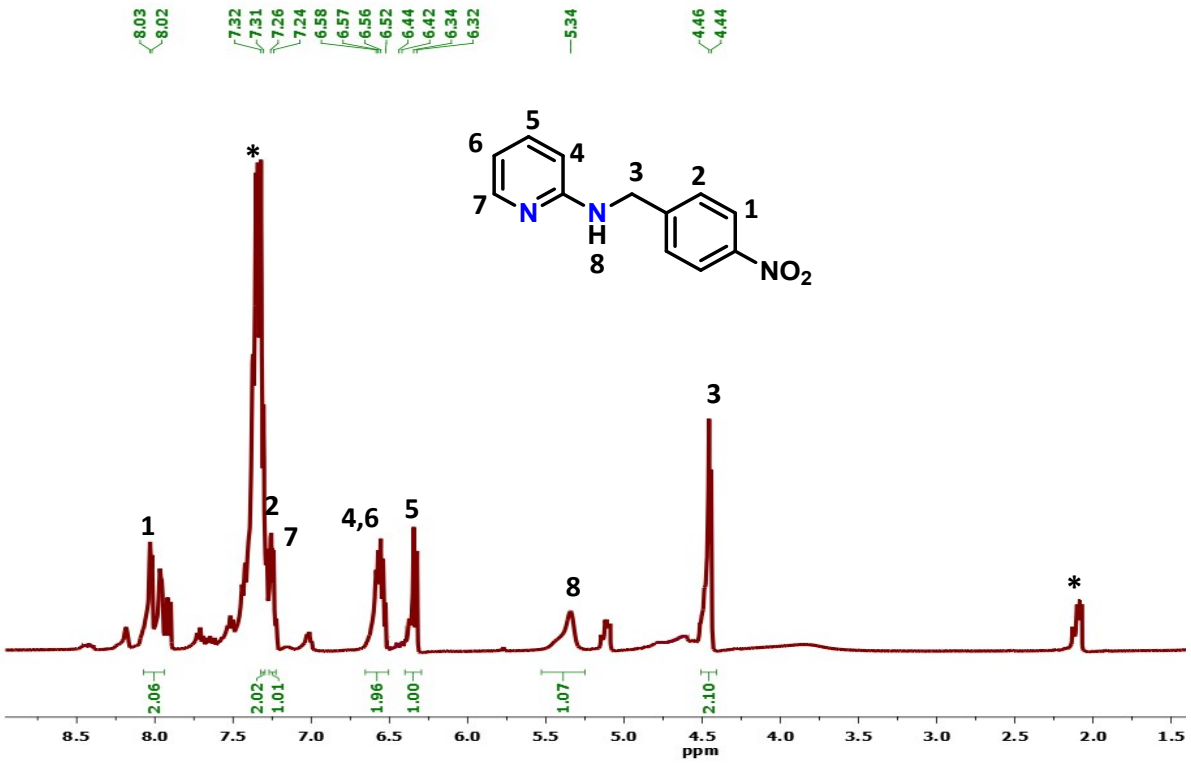

Figure S30. ^{1}H NMR (400 MHz, $CDCl_3$, 25 °C) spectrum of **4e**. Asterisk represents the residual solvents and adventitious water.

Table S1. *N*-alkylation reaction between aniline and benzyl alcohol catalyzed by various cobalt based catalysts reported in the literature.

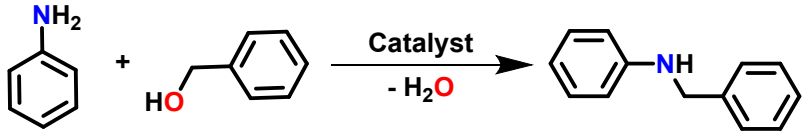

S. No.	Catalyst	Reaction Conditions	Yield (%)	Reference
1	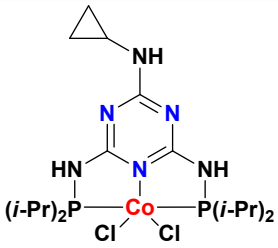	2-mol% catalyst, ^{t}BuOK, Toluene, 80 °C, 24 h	90	1
2	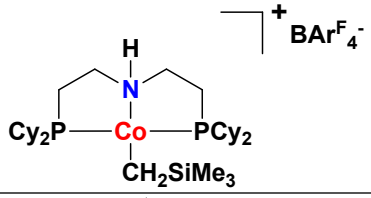	2-mol% catalyst, Toluene, Reflux (> 110 °C), 4 Å Molecular sieves	94	2
3	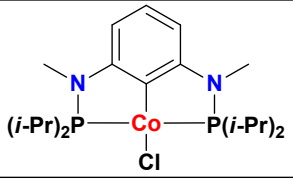	2-mol% catalyst, ^{t}BuOK, Toluene, 80 °C or 130 °C, 16 h	93	3
4	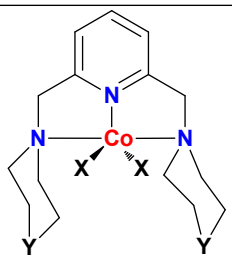 **X = Cl or Br; Y = O or NH**	5-mol% catalyst, n-octane, ^{t}BuOK, 130 – 150 °C	88	4
5	**$CoCl_2.6H_2O/PPh_3$**	5-mol% $CoCl_2.6H_2O$, 10-mol% PPh_3, ^{t}BuOK, Toluene, 130 °C, 18 h	64	5

References:

1. S. Rösler, M. Ertl, T. Irrgang and R. Kempe, *Angew. Chem. Int. Ed.,* 2015, **54**, 15046.

2. (a) G. Zhang, Z. Yin and S. Zheng, *Org. Lett.,* 2016, **18**, 300–303. (b) Z. Yin, H. Zeng, J. Wu, S. Zheng and G. Zhang, *ACS Catal.,* 2016, **6**, 6546.

3. M. Mastalir, G. Tomsu, E. Pittenauer, G. Allmaier and K. Kirchner, *Org. Lett.,* 2016, **18**, 3462.

4. S. P. Midya, J. Pitchaimani, V. G. Landge, V. Madhu and E. A. Balaraman, *Catal. Sci. Technol.,* 2018, **8**, 3469.

5. S. P. Midya, A. Mondal, A. Begum and E. A. Balaraman, *Synthesis*, 2017, **49**, 3957.

Table S2. X-ray data collection and structure refinement parameters for **1 – 3**.

	1	**2**	**3**
Formula	$C_{28}H_{21}Cl_4Co_2N_{11}O_4S_4$	$C_{13}H_{13}Cl_2CoN_5O_2S_2$	$C_{21}H_{15}Cl_2CoN_7O_2$
Formula weight	963.46	465.23	527.23
T (K)	298(2)	298(2)	273(2)
Cell system	Monoclinic	Monoclinic	Monoclinic
Space group	*C2/c*	*C*2/c	$P2_1/n$
a (Å)	21.496(3)	17.7178(10)	10.7819(15)
b (Å)	12.5372(12)	12.5889(6)	10.4395(15)
c (Å)	13.863(3)	7.9556(4)	18.083(3)
α (°)	90	90	90
β (°)	103.800(16)	100.462(5)	94.555(4)
γ (°)	90	90	90
V (Å^3)	3628.2(10)	3459.47(18)	2029.0(5)
Z	4	4	4
$\rho_{calc.}$ (mg/m^3)	1.764	1.771	1.726
μ (mm^{-1})	1.493	1.547	1.147
F (000)	1936	940	1068
Goodness-of-fit (GOF) on F^2	1.132	0.997	1.111
Final *R* indices [$I > 2\sigma(I)$][a,b]	$R_1 = 0.1225$, $wR_2 = 0.2794$	$R_1 = 0.0425$, $wR_2 = 0.0904$	$R_1 = 0.0981$, $wR_2 = 0.2367$
R indices (all data)	$R_1 = 0.1683$, $wR_2 = 0.3114$	$R_1 = 0.0614$, $wR_2 = 0.1021$	$R_1 = 0.1138$, $wR_2 = 0.2482$
CCDC No.	1995912	1995911	1995910

$R = \sum(\| Fo | - | Fc \|) / \sum | Fo |$, [b] $wR = \{\sum[w(F_o^2 - F_c^2)^2] / \sum[w(F_o^2)^2]\}^{1/2}$

Table S3. Selected distances (Å) and angles (°) for **1–3**.

Bonds	**1**	**Bonds**	**2**	**Bonds**	**3**
Co(1)-N(1)	2.050(9)	Co-N(1)	2.034(3)	Co-N(1)	2.019(6)
Co(1)-N(3)	2.204(8)	Co-N(2)	2.212(2)	Co-N(5)	2.155(6)
Co(1)-N(2)	2.225(8)	Co-N(2)$^{\#1}$	2.212(2)	Co-N(2)	2.172(6)
Co(1)-Cl(2)	2.296(3)	Co-Cl(1)	2.2804(8)	Co-Cl(1)	2.288(2)
Co(1)-Cl(1)	2.309(3)	Co-Cl(1)$^{\#1}$	2.2804(8)	Co-Cl(2)	2.324(2)
N(1)-Co(1)-N(3)	75.2(3)	N(1)-Co-N(2)	76.09(6)	N(1)-Co-N(5)	76.5(2)
N(1)-Co(1)-N(2)	75.4(3)	N(1)-Co-N(2)$^{\#1}$	76.09(6)	N(1)-Co-N(2)	76.3(3)
N(3)-Co(1)-N(2)	149.5(3)	N(2)-Co-N(2)$^{\#1}$	152.19(12)	N(5)-Co-N(2)	152.5(2)
N(1)-Co(1)-Cl(2)	112.5(3)	N(1)-Co-Cl(1)	123.26(3)	N(1)-Co-Cl(1)	121.5(2)
N(3)-Co(1)-Cl(2)	100.7(3)	N(2)-Co-Cl(1)	98.29(6)	N(5)-Co-Cl(1)	99.39(19)
N(2)-Co(1)-Cl(2)	97.8(2)	N(2)$^{\#1}$-Co-Cl(1)	96.86(6)	N(2)-Co-Cl(1)	97.63(19)
N(1)-Co(1)-Cl(1)	137.2(3)	N(1)-Co-Cl(1)$^{\#1}$	123.26(3)	N(1)-Co-Cl(2)	134.3(2)
N(3)-Co(1)-Cl(1)	97.3(2)	N(2)-Co-Cl(1)$^{\#1}$	96.86(6)	N(5)-Co-Cl(2)	98.60(19)
N(2)-Co(1)-Cl(1)	98.7(3)	N(2)$^{\#1}$-Co-Cl(1)$^{\#1}$	98.28(6)	N(2)-Co-Cl(2)	98.0(2)
Cl(2)-Co(1)-Cl(1)	110.35(14)	Cl(1)-Co-Cl(1)$^{\#1}$	113.49(6)	Cl(1)-Co-Cl(2)	104.14(9)
C(10)-N(3)-Co(1)	114.3(6)	C(3)$_{\#1}$-N(1)-Co	120.23(16)	C(5)-N(2)-Co	124.6(5)
C(11)-N(3)-Co(1)	129.1(7)	C(3)-N(1)-Co	120.23(16)	C(4)-N(2)-Co	115.8(5)
C(4)-N(2)-Co(1)	116.1(7)	C(5)-N(2)-Co	128.61(18)	C(15)-N(5)-Co	126.4(5)
C(5)-N(2)-Co(1)	125.4(7)	C(4)-N(2)-Co	114.11(17)	C(14)-N(5)-Co	115.2(5)
C(9)-N(1)-Co(1)				C(13)-N(1)-Co	119.8(5)
C(3)-N(1)-Co(1)				C(3)-N(1)-Co	120.2(5)

Symmetry transformations used to generate equivalent atoms for complex **2** (#1): -x+1, y, -z+1/2.

Table S4. Literature values of the Co-Cl distances for a few selected Co(II) complexes.

S. No.	Chemical structure	Distance (Å)	Reference
1	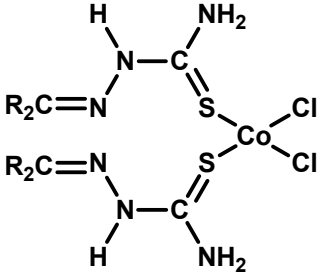	Co – Cl = 2.256	B. Sen, H. K. Kalhan, V. Demir, E. E. Güler, H. A. Kayali and E. Subasi, *Mat. Sci. Engin.:C*, 2019, ***98***, 550.
2	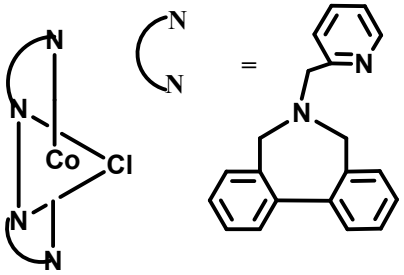	Co – Cl = 2.334	S. Sabiah, B. Varghese and N. N. Murthy, *J. Chem. Crystallogr.*, 2006, **36**, 147.
3	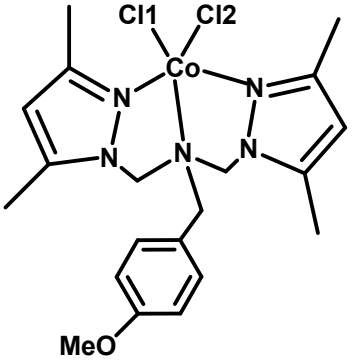	Co-Cl1 = 2.231 Co-Cl2 = 2.261	I. Banerjee, A. Jana, S. Singh, J. Marek, E. del Barco and M. Ali, *Polyhedron*, 2013, **66**, 162.
4	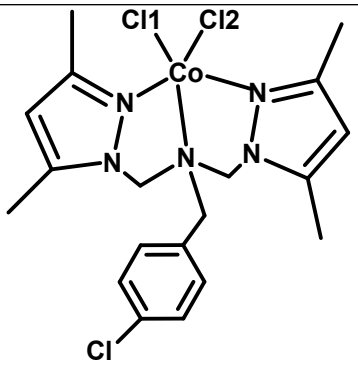	Co-Cl1 = 2.069 Co-Cl2 = 2.206	I. Banerjee, A. Jana, S. Singh, J. Marek, E. del Barco and M. Ali, *Polyhedron*, 2013, **66**, 162.

Table S5. *N*-alkylation reaction between 2-aminopyridine and benzyl alcohol by using an equimolar mixture of a pro-ligand/ligand (H_2L^1 – H_2L^9) and $CoCl_2$ as the catalyst (5-mol%).

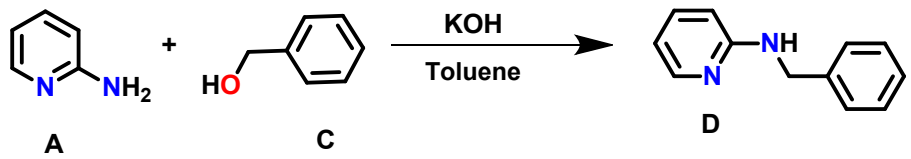

A C D

S. No.	Ligand	Metal Salt	Gas Chromatograph Peak Area		Yield (%)	Reference
			A	D		
1	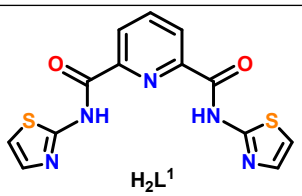 H_2L^1	$CoCl_2$	28123	195470	87	This work
2	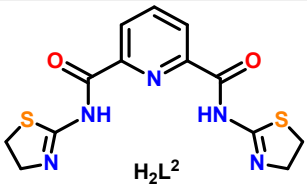 H_2L^2	$CoCl_2$	52449	132643	71	This work
3	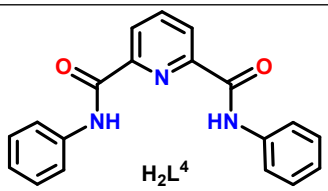 H_2L^4	$CoCl_2$	36946	5672	13	1
4	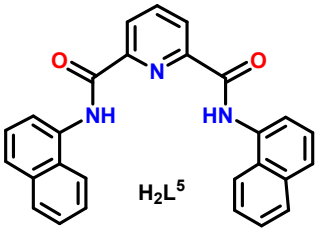 H_2L^5	$CoCl_2$	191648	65069	25	1
5	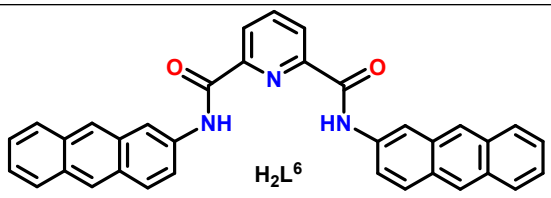 H_2L^6	$CoCl_2$	91486	37138	28	1

6	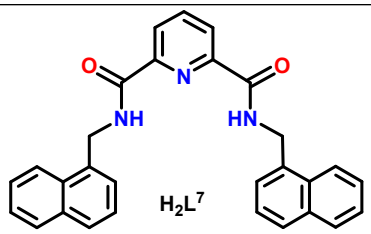	**$CoCl_2$**	63981	13153	17	2
7	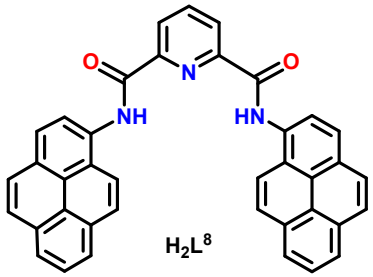	**$CoCl_2$**	37760	5273	12	3
8	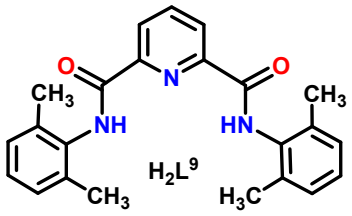	**$CoCl_2$**	105162	11439	9	4

References:

1. P. Kumar, V. Kumar and R. Gupta, *RSC Adv.*, 2015, **5**, 97874-97882.

2. P. Kumar, V. Kumar, S. Pandey and R. Gupta, *Dalton Trans.*, 2018, **47**, 9536 – 9545.

3. H. Goyal, S. Pachisia and R. Gupta, *Cryst. Growth Des.*, 2020, **20**, 6117 – 6128.

4. J. Tehranchi, P. J. Donoghue, C. J. Cramer and W. B. Tolman, *Eur. J. Inorg. Chem.*, 2013, 4077 – 4084.